A One-Dimensional Array of Clusters: $Na_2Mo_6Cl_8(O_2CC_5H_4FeCp)_6 \cdot CH_3OH$

Nicholas Prokopuk and Duward F. Shriver*

Department of Chemistry, Northwestern University, Evanston, Illinois 60208-3113

Received July 2, 1997[⊗]

Reaction of $Na_2Mo_6Cl_8(OMe)_6$ with $CpFeC_5H_4CO_2H$ produces the new cluster $Na_2Mo_6Cl_8(O_2CC_5H_4FeCp)_6 \cdot HOCH_3$, which consists of a novel one-dimensional chain from the interactions of the Na^+ ions with the carboxylate ligands of adjacent clusters. Coordination of the Na^+ cations to the carboxylate ligands is reflected in the vibrational spectroscopy of the sodium salt of $[Mo_6Cl_8(O_2CC_5H_4FeCp)_6]^{2-}$. Both the $[Mo_6Cl_8]^{4+}$ and ferrocenecarboxylate groups are redox active. Voltammetry of the sodium salt of the cluster in DMSO reveals that the ferroceniumcarboxylate ligands dissociate with a rate constant of $k = 0.6\ s^{-1}$. Crystallographic data for $Na_2Mo_6Cl_8(O_2CC_5H_4FeCp)_6 \cdot CH_3OH$: monoclinic space group, $P2_1/c$ (No. 14), $a = 13.175(3)$ Å, $b = 25.148(8)$ Å, $c = 11.264(2)$ Å, $\beta = 92.10(2)°$, $V = 3729(1)$ Å^3, $Z = 2$.

Introduction

There is current interest in the solid state chemistry of molecularly derived solids with extended linkages.[1−5] A number of solids have been derived through solution chemistry in which soluble metal complexes are linked together by bridging ligands, the most notable example being Prussian blue.[6−12] Substantially fewer examples are known in which soluble metal cluster fragments are connected into extended arrays. Two recent developments in this area are the one- and two-dimensional bonding in three-dimensional solids of polyoxoanions bridged by single metal complexes[13] and three-dimensional ensembles of the metal halide clusters $[Nb_6X_zY_6]^{4+}$ (X = Cl, Br; Y = NCS, N_3) linked through cation−ligand interactions.[14−16] Interest in ordered solids comprising the group 5 and 6 metal halide clusters $[M_6Cl_z]^{n+}$ (M = Mo, W, $z = 8$; M = Nb, Ta, $z = 12$) arises from the novel electrochemical and photophysical properties of the molecular species. A number of strategies have been used to combine the properties of these clusters with solids, including adsorption of $[Mo_6Cl_8]^{4+}$ by polymeric materials[17−21] and intercalation of $[M_6Cl_{12}]^{2+}$ and $[Mo_6Cl_8]^{4+}$ into layered aluminosilicates.[21,22] Synthesis of ordered arrays using ligands to bridge metal clusters remains a challenging but viable method for creating new materials that incorporate properties of the molecular clusters.

Chart 1

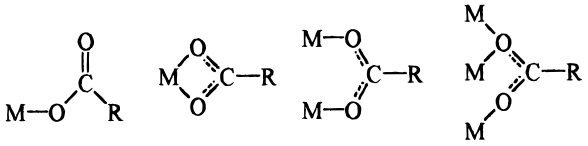

Carboxylate ligands are known to bridge metal centers, and they are potential candidates for the formation of extended arrays. RCO_2^- ligands coordinate[23−26] to metal clusters in several different configurations (See Chart 1.) The only known clusters containing the $[Mo_6Cl_8]^{4+}$ core with carboxylate ligands, $[Mo_6Cl_8(O_2CR)_6]^{2-}$ (R = CF_3, CH_3), have been isolated as tetra butyl ammonium salts.[27,28] In both compounds the RCO_2^- moiety binds in a unidentate fashion, **A**, as determined by vibrational spectroscopy. Herein we report the synthesis of the title compound from the reaction of the organometallic carboxylic acid $CpFeC_5H_4CO_2H$ with $Na_2Mo_6Cl_8(OCH_3)_6$. The interactions of the redox-active carboxylic group with the molybdenum chloride core and the sodium counterions are reported, and the X-ray structure reveals a novel one-dimensional chain of clusters.

Experimental Section

All manipulations were performed under prepurified N_2 atmosphere using standard Schlenk and syringe techniques. The solvents methanol, dimethylformamide, dimethyl sulfoxide, acetonitrile, and ether were

[⊗] Abstract published in *Advance ACS Abstracts,* November 1, 1997.

(1) Smart, L.; Moore, E. *Solid State Chemistry*; Chapman and Hall: London, 1992.
(2) Cheetham, A. K.; Day, P. In *Solid State Chemistry*; Cheetham, A. K., Day, P., Eds.; Clarendon Press: Oxford, U.K., 1992.
(3) Thomas, J. M. *Angew. Chem.* **1988**, *27*, 1673−1691.
(4) Suib, S. L. *Chem. Rev.* **1993**, *93*, 803−826.
(5) DiSalvo, F. J. *Science* **1990**, *247*, 649.
(6) Keggin, J. F.; Miles, F. D. *Nature* **1936**, *137*, 577−578.
(7) Soma, T.; Yuge, H.; Iwamoto, T. *Angew. Chem., Int. Ed. Engl.* **1994**, *33*, 1665−1666.
(8) Nishikiori, S.; Iwamoto, T.; Yoshino, Y. *Bull. Chem. Soc. Jpn*. **1980**, *53*, 2236−2240.
(9) Soma, T.; Iwamoto, T. *Chem. Lett.* **1995**, 271−272.
(10) Kim, J.; Whang, D.; Koh, Y. -S.; Kim, K. *J. Chem. Soc., Chem. Commun.* **1994**, 637−638.
(11) Kim, J.; Whang, D.; Lee, J.; Kim, K. *J. Chem. Soc., Chem. Comm.* **1993**, 1400−1403.
(12) Real, J. A.; Andrér, E.; Muñoz, M. C.; Julve, M.; Granier, T.; Bousseksou, A.; Varret, F. *Science* **1995**, *268*, 265−267.
(13) DeBord, J. R. D.; Haushalter, R. C.; Meyer, L. M.; Rose, D. J.; Zapf, P. J.; Zubieta, J. *Inorg. Chim. Acta* **1997**, *256*, 165−168.
(14) Reckeweg, O.; Meyer, H.-J. *Z. Naturforsch.* **1995**, *50B*, 1377−1381.
(15) Meyer, H.-J. *Z. Anorg. Allg. Chem.* **1995**, *621*, 921−924.
(16) Reckeweg, O.; Meyer, H.-J. *Z. Anorg. Allg. Chem.* **1996**, *622*, 411−416.
(17) Robinson, L. M.; Lu, H.; Hupp, J. T.; Shriver, D. F. *Chem. Mater.* **1995**, *7*, 43−49.
(18) Jackson, J. A.; Newsham, M. D.; Worsham, C.; Nocera, D. G. *Chem. Mater.* **1996**, *8*, 558−564.
(19) Golden, J. H.; Deng, H.; DiSalvo, F. J.; Frechet, J. M.; Thompson, P. M. *Science* **1995**, *268*, 1463−1466.
(20) Robinson, L. M.; Shriver, D. F. *Coord. Chem. Rev.* **1996**, *37*, 119−129.
(21) Christiano, S. P.; Wang, J.; Pinnavaia, T. J. *Inorg. Chem.* **1985**, *24*, 1222−1227.
(22) Christiano, S. P.; Pinnavaia, T. J. *J. Solid State Chem.* **1986**, *64*, 232−239.
(23) Cannon, R. D.; White, R. P. *Prog. Inorg. Chem.* **1988**, *36*, 195−298.
(24) Cotton, F. A.; Duraj, S. A.; Roth, W. J. *Inorg. Chem.* **1984**, *23*, 4042−4045.
(25) Cotton, F. A.; Lewis, G. E.; Mott, G. N. *Inorg. Chem.* **1983**, *22*, 1825−1827.
(26) Koh, Y. B.; Christoph, G. G. *Inorg. Chem.* **1979**, *18*, 1122−1128.

S0020-1669(97)00816-1 CCC: $14.00

dried over MgI_2, 4-Å molecular sieves, 4-Å molecular sieves, CaH_2, and sodium/benzophenone, respectively, and distilled prior to use (vacuum-distilled in the case of dimethyl sulfoxide and dimethylformamide). $Na_2Mo_6Cl_8(OCH_3)_6$ was prepared by the method of Johnston *et al.*[27] 4,7,13,16,21,24-Hexaoxa-1,10-diazabicyclo[8.8.8]hexacosane (crypt) (Aldrich) was dried under vacuum, and ferrocenecarboxylate (Aldrich) was used as received. Tetrabutylammonium tetrafluoroborate (Aldrich) was recrystallized from methanol and diethyl ether.

Synthesis of $Na_2Mo_6Cl_8(O_2CC_5H_4FeCp)_6$ and $(cryptNa)_2Mo_6Cl_8(O_2CC_5H_4FeCp)_6$. To a solution of $Na_2Mo_6Cl_8(OCH_3)_6$ (0.067 mmol) in 5 mL of methanol was added 10 mL of methanol containing 0.44 mmol of $HO_2CC_5H_4FeCp$. The resulting orange suspension was concentrated to ca. 2 mL and layered with diethyl ether to induce further precipitation of the product. The solids were collected by filtration, washed with a 5 mL portion of ether, and dried *in vacuo*. Total yield: 65 mg (43%). Anal. Calcd (found) for $C_{66}H_{54}Cl_8Fe_6Mo_6Na_2$: C, 34.78 (35.93); H, 2.39 (2.31). The cryptated salt $(cryptNa)_2Mo_6Cl_8(O_2CC_5H_4FeCp)_6$ was prepared by addition of $HO_2CC_5H_4FeCp$ to a solution of crypt and $Na_2Mo_6Cl_8(OCH_3)_6$ in a 2:1 molar ratio. The resulting suspension was then worked up in the same manner as the sodium salt. Anal. Calcd (found) for $C_{102}H_{126}N_4O_6Cl_8Fe_6Mo_6Na_2$: C, 40.40 (40.86); H, 4.19 (4.14); N, 1.85 (1.75).

Instrumentation. IR spectra were determined for Nujol and Fluorolube mulls of the solid between KBr plates or as solutions in 0.1 mm path length CaF_2 solution cells using a Bomem MB-100 FT-IR set at 2-cm^{-1} resolution. Raman spectra were collected at 2-cm^{-1} resolution on a Bio-R FT Raman spectrometer with a Nd:YAG laser at 90 mW power. UV−visible spectra were obtained on a Varian Cary 1E UV−visible spectrometer as solutions in cells modified for air-sensitive samples. Fluorescence measurements were performed on a Photon Technology International (PTI) QM-2 fluorimeter with a 75 W xenon lamp. Cyclic voltammograms were obtained with a Bioanalytical Systems 100B electrochemical analyzer. A Pt-disk working electrode and a Pt-foil counter electrode were employed. All potentials were measured against a (BAS) Ag/AgCl reference electrode. Elemental analyses were performed by Oneida Research Services, Inc., Whitesboro, NY.

X-ray Crystal Structure of $Na_2Mo_6Cl_8(O_2CC_5H_4FeCp)_6$. Red-orange crystals of $Na_2Mo_6Cl_8(O_2CC_5H_4FeCp)_6$ were grown by slow diffusion of diethyl ether into a solution of the cluster in methanol. A hexagonal platelike crystal (approximate dimensions of 0.23 × 0.17 × 0.04 mm) immersed in Paratone-N (Exxon) was mounted on a glass fiber and transferred to an Enraf-Nonius CAD4 diffractometer. Data were collected at −120 °C with graphite-monochromated Mo−Kα radiation. A set of 25 carefully centered reflections were used to obtain a least-squares-refined primitive monoclinic cell. The space group was determined to be $P2_1/c$ (No. 14) by the systematic absences. The data were collected using the $\omega-\theta$ scan technique to a maximum 2θ value of 48.9°. Of the 6705 reflections collected, 6386 were unique and 2665 observed ($I > 3.00\sigma(I)$). The intensities of three representative reflections were measured every 90 min of X-ray exposure, and no appreciable decay was observed. A summary of the crystallographic data is given in Table 1. An analytical absorption correction was applied, resulting in transmission factors from 0.70 to 0.91. The data were corrected for Lorentz and polarization effects.

Calculations were performed using TEXSAN crystallographic software (Molecular Structure Corp.) by direct methods (SHELXS86). Neutral-atom scattering factors[29] and anomalous dispersion effects[30] were taken from the literature. The Mo, Fe, Cl, and Na atoms were refined anisotropically, and isotropic thermal parameters were used for the remaining non-hydrogen atoms. Hydrogen atoms were included in idealized positions (except for those on the solvent molecule) but not refined. The final cycle of full-matrix least-squares refinement converged with an R value of 0.068 ($R_w = 0.061$). The maximum and minimum peaks in the final difference Fourier map corresponded to 1.62 and −1.34 $e^-/Å^3$, respectively, and were located in the vicinity of the metal positions.

Table 1. Crystal Data for $Na_2Mo_6Cl_8(O_2CC_5H_4FeCp)_6 \cdot 2CH_3OH$

empirical formula	$Na_2Mo_6Cl_8C_{68}O_{14}Fe_6H_{60}$
M	2341.54
crystal size, mm	0.32 × 0.17 × 0.04
crystal system	monoclinic
space group	$P2_1/c$ (No. 14)
a, Å	13.175(3)
b, Å	25.148(8)
c, Å	11.264(2)
β, deg	92.10(2)
V, Å^3	3729(1)
Z	2
d(calcd), g/cm^3	2.085
μ(Mo Kα), cm^{-1}	24.57
T (°C)	−120
$R(F)^a$	0.068
$R_w(F)^b$	0.061

^{a} $R(F) = \sum||F_o| - |F_c||/\sum|F_o|$. ^{b} $R_w(F) = [\sum w(|F_o| - |F_c|)^2/\sum wF_o^2]^{1/2}$.

Results and Discussion

The sodium and sodium cryptate salts of the mixed-metal cluster $[Mo_6Cl_8(O_2CC_5H_4FeCp)_6]^{2-}$ are readily synthesized from the appropriate salt of $[Mo_6Cl_8(OMe)_6]^{2-}$ and ferrocenecarboxylic acid, $HO_2CC_5H_4FeCp$. $[Mo_6Cl_8(OMe)_6]^{2-}$ reacts readily with proton sources and has been used as a starting material for generating clusters with aromatic alkoxide ($^-$OAr) ligands, $[Mo_6Cl_8(OAr)_6]^{2-}$.[31,32] The sodium and the sodium cryptate salt of the new ferrocenecarboxylate cluster have solubilities comparable to those of other[31−33] $[Mo_6Cl_8]^{4+}$ clusters with similar counterions: insolubility in CH_3CN, slight solubility in methanol, and high solubility in dimethylformamide and dimethyl sulfoxide. Cyclic voltammetry of $(cryptNa)_2[Mo_6Cl_8(O_2CC_5H_4FeCp)_6]$ indicates that the ferrocenecarboxylate ligands are not displaced by either DMF or DMSO. Neither the sodium nor the sodium cryptate salt is air or light sensitive in the solid state.

Single-crystal X-ray diffraction reveals the structure of $Na_2Mo_6Cl_8(O_2CC_5H_4FeCp)_6$ to contain a $[Mo_6Cl_8]^{4+}$ core on a center of inversion and six attached $^-O_2CC_5H_4FeCp$ ligands. A diagram of the anion is shown in Figure 1. The crystallographic data are given in Table 1, positional parameters in Table 2, and selected bond lengths and angles in Table 3. The metal atoms are numbered Mo(1)−Mo(3) and Fe(1)−Fe(3) with the iron atom numbers corresponding to the molybdenum atom of the appropriate ferrocenecarboxylate. Thus the iron atom in the ferrocenecarboxylate bound to Mo(1) is Fe(1). Oxygen and carbon atoms are numbered so the atoms of the $^-O_2CC_5H_4FeCp$ moiety attached to Mo(1) are numbered first with the oxygen atoms O(1) and O(2) and the carbon atoms C(1)−C(11). The C and O atoms of the $^-O_2CC_5H_4FeCp$ ligand on Mo(2) are labeled next followed by those of the ligand on Mo(3). O(1), O(3), and O(5) bind the carboxyl groups to the molybdenum framework. Atoms O(7) and C(34) are those of the methanol solvent molecule of the crystal structure. The structure of the $[Mo_6Cl_8]^{4+}$ core is essentially identical to other structures containing the molybdenum chloride cluster.[27,28,31,32,34−38] Each

(27) Johnston, D. H.; Gaswick, D. C.; Lonergan, M. C.; Stern, C. L.; Shriver, D. F. *Inorg. Chem.* **1992**, *31*, 1869−1873.
(28) Harder, K.; Preetz, W. *Z. Anorg. Allg. Chem.* **1992**, *612*, 97−100.
(29) Cromer, D. T.; Waber, J. T. *International Tables for X-ray Crystallography*; The Kynoch Press: Birmingham, England, 1974; Vol. IV.
(30) Creagh, D. C.; McAuley, W. J. *International Tables for Crystallography*; Kluwer Academic Publishers: Boston, MA, 1992; Vol. C.
(31) Perchenek, N.; Simon, A. *Z. Anorg. Allg. Chem.* **1993**, *619*, 103−108.
(32) Perchenek, N.; Simon, A. *Z. Anorg. Allg. Chem.* **1993**, *619*, 98−102.
(33) Nannelli, P.; Block, B. P. *Inorg. Chem.* **1968**, *7*, 2423−2426.
(34) Johnston, D. H.; Stern, C. L.; Shriver, D. F. *Inorg. Chem.* **1993**, *32*, 5170−5175.
(35) Saito, T.; Nishida, M.; Yamagata, T.; Yamagata, Y.; Yamaguchi, Y. *Inorg. Chem* **1986**, *25*, 1111−1117.

Table 2. Positional Parameters and B_{eq} Values for $Na_2Mo_6Cl_8(O_2CC_5H_4FeCp)_6 \cdot 2CH_3OH$

atom	*x*	*y*	*z*	B_{eq},[a] Å^2
Mo(l)	0.1358(2)	0.00831(9)	0.9702(2)	1.13(5)
Mo(2)	−0.0302(2)	0.05915(9)	0.9091(2)	1.08(5)
Mo(3)	−0.0168(2)	−0.04203(9)	0.8676(2)	1.06(5)
Fe(l)	0.4679(3)	0. 1318(1)	0.9402(3)	2.22(9)
Fe(2)	−0.1729(3)	0.2453(1)	0.6641(3)	1.72(8)
Fe(3)	−0.2762(3)	−0.1412(2)	0.5498(3)	2.20(9)
Cl(1)	0.0852(4)	0.0241(2)	0.7607(5)	1.4(l)
Cl(2)	0.1164(4)	0.1044(2)	1.0117(5)	1.4(1)
Cl(3)	−0.1728(4)	0.0084(2)	0.8159(5)	1.5(1)
Cl(4)	0. 1427(4)	−0.0882(2)	0.9302(5)	1.4(l)
Na	−0.1069(7)	0.0355(4)	0.5034(8)	2.3(2)
O(1)	0.286(1)	0.0193(6)	0.951(1)	2.1(3)
O(2)	0.337(1)	0.0186(7)	0.763(2)	3.8(4)
O(3)	−0.0560(10)	0.1297(5)	0.815(1)	1.0(3)
O(4)	−0.099(1)	0. 1009(7)	0.631(1)	2.7(4)
O(5)	−0.043(1)	−0.0942(6)	0.726(1)	1.6(3)
O(6)	−0.056(1)	−0.0464(6)	0.563(1)	2.1(3)
O(7)	−0.256(1)	0. 0461(7)	1.401(2)	3.7(4)
C(1)	0.356(2)	0.029(1)	0.872(2)	3.1(6)
C(2)	0.450(2)	0.0512(9)	0.916(2)	1.7(5)
C(3)	0.530(2)	0.070(1)	0.843(2)	2.7(6)
C(4)	0.606(2)	0.0936(10)	0.920(2)	2.0(5)
C(5)	0.572(2)	0.089(1)	1.044(2)	2.6(6)
C(6)	0.474(2)	0.0638(10)	1.038(2)	2.2(5)
C(7)	0.414(2)	0.188(1)	0.818(2)	3.0(6)
C(8)	0.332(2)	0.163(1)	0.881(2)	2.4(5)
C(9)	0.351(2)	0.174(1)	1.005(2)	3.1(6)
C(10)	0.443(2)	0.203(1)	1.024(2)	2.7(6)
C(11)	0.486(2)	0.2114(10)	0.904(2)	2.7(5)
C(12)	−0.070(2)	0.139(1)	0.705(2)	2.8(6)
C(13)	−0.059(2)	0.1920(9)	0.660(2)	1.0(4)
C(14)	−0.028(2)	0.2355(9)	0.730(2)	0.9(4)
C(15)	−0.038(2)	0.281(1)	0.658(2)	2.4(5)
C(16)	−0.069(2)	0.2676(9)	0.544(2)	1.3(4)
C(17)	−0.083(2)	0.2119(9)	0.546(2)	1.6(5)
C(18)	−0.265(2)	0.247(1)	0.801(2)	2.6(5)
C(19)	−0.273(2)	0.297(1)	0.742(3)	4.1(7)
C(20)	−0. 306(2)	0.283(1)	0.626(2)	2.8(6)
C(21)	−0.320(2)	0.230(l)	0.617(2)	3.0(6)
C(22)	−0.295(2)	0.2047(10)	0.725(2)	2.3(5)
C(23)	−0.073(2)	−0.088(1)	0.620(2)	2.2(5)
C(24)	−0.126(2)	−0.1344(10)	0.560(2)	1.7(5)
C(25)	−0.155(2)	−0.1791(9)	0.624(2)	1.4(5)
C(26)	−0.205(2)	−0.2136(10)	0.539(2)	2.6(5)
C(27)	−0.208(2)	−0.189(1)	0.429(2)	3.7(6)
C(28)	−0.161(2)	−0.137(1)	0.439(2)	3.6(6)
C(29)	−0.354(2)	−0.102(1)	0.677(3)	4.2(7)
C(30)	−0.345(2)	−0.069(1)	0.579(3)	4.3(7)
C(31)	−0.391(2)	−0.091(1)	0.484(3)	4.1(7)
C(32)	−0.430(2)	−0.140(1)	0.516(3)	4.3(7)
C(33)	−0.407(2)	−0.148(1)	0.638(3)	4.3(7)
C(34)	−0.345(2)	0.075(1)	1.443(3)	5.7(8)

[a] $B_{eq} = {}^8/_3\pi^2(U_{11}(aa^*)^2 + U_{22}(bb^*)^2 + U_{33}(cc^*)^2 + 2U_{12}aa^*bb^* \cos\gamma + 2U_{13}aa^*cc^* \cos\beta + 2U_{23}bb^*cc^* \cos\alpha)$.

carboxylate moiety interacts with only one Mo center of the Mo_6 octahedron through a single oxygen atom. The average Mo−O distance is 2.06 Å. This distance is similar to other Mo−O distances observed for $[Mo_6Cl_8L_6]^{2-}$ clusters in which L is an anionic oxygen donor ligand such as $^-OSO_2CF_3$ (d(Mo−O) = 2.123 Å)[27] and ^-OMe (d(Mo−O) = 2.046 Å).[31]

An interesting feature of the structure is the position of sodium ion relative to the carboxylic groups. Of the six carboxylate ligands on each cluster, only three are crystallographically unique. Two of these $^-O_2CC_5H_4FeCp$ units have one oxygen atom coordinated to the $[Mo_6Cl_8]^{4+}$ core and the second oxygen coordinated to the sodium counterions. One of these carboxylate

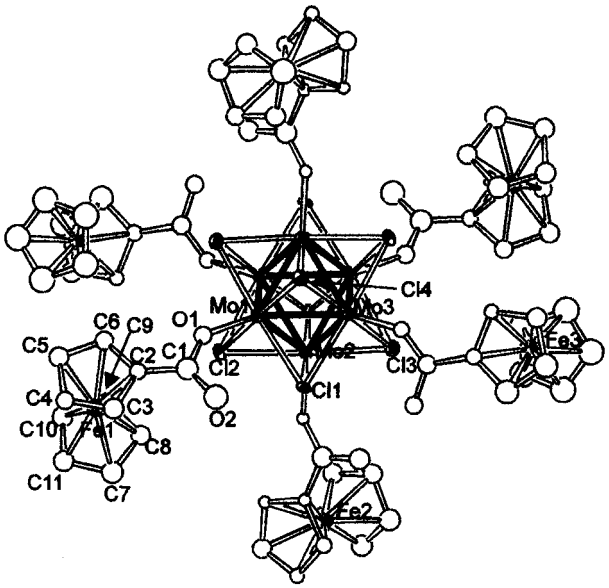

Figure 1. Diagram of the anion of $Na_2Mo_6Cl_8(O_2CC_5H_4FeCp)_6$. Thermal ellipsoids are at 50% probability. See text for labeling scheme.

Table 3. Selected Interatomic Distances (Å) and Bond Angles (deg) for $Na_2Mo_6Cl_8(O_2CC_5H_4FeCp)_6 \cdot 2CH_3OH$[a]

Interatomic Distances			
Mo(1)−Mo(2)	2.604(3)	Mo(1)−Mo(3)	2.609(3)
Mo(2)−Mo(3)	2.604(3)	Mo(1)−Cl(1)	2.461(6)
Mo(2)−Cl(1)	2.464(6)	Mo(3)−Cl(1)	2.477(6)
Mo(1)−O(1)	2.02(1)	Mo(2)−O(3)	2.09(1)
Mo(3)−O(5)	2.08(1)	O(1)−C(1)	1.32(3)
C(1)−O(2)	1.27(3)	C(1)−C(2)	1.43(3)
C(2)−C(3)	1.45(3)	C(3)−C(4)	1.43(3)
C(4)−C(5)	1.49(3)	C(5)−C(6)	1.44(3)
C(6)−C(2)	1.44(3)	C(2)−Fe(1)	2.06(2)
C(3)−Fe(1)	2.08(3)	C(4)−Fe(1)	2.08(2)
C(5)−Fe(1)	2.08(3)	C(6)−Fe(1)	2.04(2)
C(7)−Fe(1)	2.08(3)	C(8)−Fe(1)	2.05(2)
C(9)−Fe(1)	2.02(3)	C(10)−Fe(1)	2.06(3)
C(11)−Fe(1)	2.06(3)	Na−O(4)	2.19(2)
Na−O(6)	2.26(2)	Na*−(O6)	2.32(2)
Na−O(7)	2.25(2)		

Angles			
Mo(1)−O(1)−C(1)	143(1)	Mo(2)−O(3)−C(12)	131(1)
Mo(3)−O(5)−C(23)	133(1)	O(1)−C(1)−O(2)	119(2)
O(3)−C(12)−O(4)	121(2)	O(5)−C(23)−O(6)	121(2)
C(1)−C(2)−Fe(1)	121(1)	C(12)−C(13)−Fe(2)	121(1)
C(23)−C(24)−Fe(3)	122(1)		

[a] An asterisk indicates an atom related by a center of inversion.

groups, coordinated to Mo(3), bridges two sodium ions with d(Na−O(6)) and d(Na*−O(6)) of 2.26 and 2.32 Å, respectively. The second carboxylate group coordinates to only one sodium ion (d(Na−O(4)) of 2.19 Å) in addition to the Mo(2) center. The third $^-O_2CC_5H_4FeCp$ (Fe(1)) ligand, which does not coordinate to a Na^+ ion, is terminally bound to a single Mo atom. Unidentate **A**, bridging **C**, and tridentate **D** coordination modes of the carboxylate ligand are all observed in the structure of $Na_2Mo_6Cl_8(O_2CC_5H_4FeCp)_6$, Chart 1. The Na^+ ions are related by a center of inversion and each is coordinated to a total of three carboxylate groups (one from a neighboring cluster) and one methanol molecule, Figure 2. Na−O distances in this structure are much shorter than those of an 8-coordinated sodium cryptate where d(Na−O) values range from 2.492 to 2.561 Å.[32] The short Na−O distances indicate strong interactions between the cluster-bound carboxylate and the bridging Na^+ cations. These interactions create a one-dimensional chain of $[Mo_6Cl_8(O_2CC_5H_4FeCp)_6]^{2-}$ clusters, Figure 3. Low-dimen-

(36) Guirauden, A.; Johannsen, I.; Batail, P.; Coulon, C. *Inorg. Chem.* **1993**, *32*, 2446−2452.
(37) Ehrlich, G. M.; Warren, C. J.; Haushalter, R. C.; DiSalvo, F. J. *Inorg. Chem.* **1995**, *34*, 4284−4286.
(38) Preetz, W.; Harder, K.; von Schnering, H. G.; Kliche, G.; Peters, K. *J. Alloys Compd* **1992**, *183*, 413−429.

Table 4. Stretching Frequencies for ν(C═O) and ν(C−O) for Ferrocenecarboxylate Complexes

	ν(C═O)[a]	ν(C−O)[a]
$Na_2Mo_6Cl_8(O_2CC_5H_4FeCp)_6$	1554,[b] 1582 (sh), 1606	1333, 1382
	1573,[e] 1607,[e] 1623[e]	1338,[e] 1383,[e] 1401[e]
$(cryptNa)_2Mo_6Cl_8(O_2CC_5H_4FeCp)_6$	1589 (sh),[b] 1609, 1627(sh)	1312, 1360, 1375, 1329[e]
	1634[e]	1375,[e] 1392[e]
$Na_2Mo_6Cl_8(O_2CC_5H_4FeCp)_6$[c]	1617 (sh), 1625, 1634 (sh)	
$(cryptNa)_2Mo_6Cl_8(O_2CC_5H_4FeCp)_6$[c]	1617 (sh), 1625, 1633 (sh)	
$CpFeC_5H_4CO_2H$	1658[b]	1281
	1634[d,e]	1285[e]
$CpFeC_5H_4CO_2H$[c]	1701	

[a] All values are reported in cm^{-1}; sh indicates a shoulder. [b] Samples taken as mulls. [c] Samples taken in DMSO. [d] Due to hydrogen bonding in solid ferrocenecarboxylic acid (Iwai, K.; Katada, M.; Motoyama, I.; Sano, H. *Bull. Chem. Soc. Jpn.* **1987**, *60*, 1961−1966), two ν(C═O) bands are observed. [e] Raman shift.

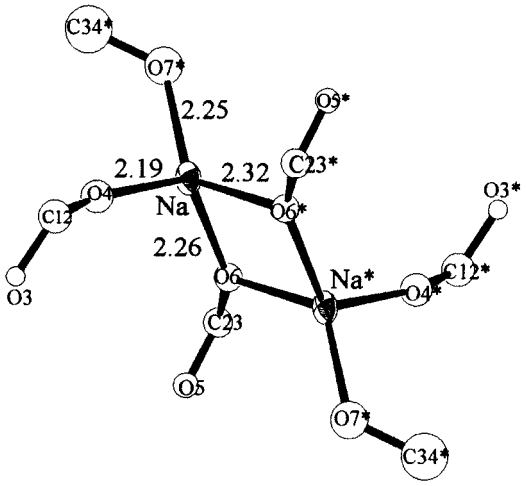

Figure 2. Diagram of the coordination environment about the sodium ions of $Na_2Mo_6Cl_8(O_2CC_5H_4FeCp)_6$. Pendant ferrocenyl groups of C(12) and C(23) are omitted for clarity. C(34) and O(7) comprise the methanol molecule in the crystal structure. Asterisks indicate atoms related by an inversion center. Atom labels are outlined in the text. All bond lengths are in angstroms.

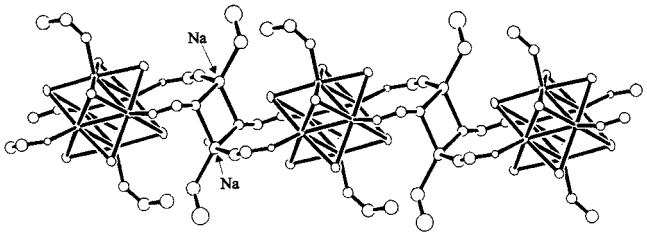

Figure 3. Display of the linear chains of the $[Mo_6Cl_8]^{4+}$ cluster connected through bridging carboxylate ligands and sodium ions. The ferrocenyl moieties of the carboxylate groups are omitted for clarity.

sional extended solids containing octahedral metal halide clusters have previously been made via solid state synthesis.[39]

Vibrational spectroscopy of the crystalline sodium and sodium cryptate salts of $[Mo_6Cl_8(O_2CC_5H_4FeCp)_6]^{2-}$ reveals large differences in the ν(C═O) and ν(C−O) region, reflecting differences in the carboxylate−cation interaction, Table 4. An increase in the ν(C═O) and lowering of the ν(C−O) bands are observed upon encapsulating the sodium ion with the cryptand as expected for the decreasing interaction between the carboxylate oxygens and alkali metal centers.[40] IR spectra for the two salts in solution have identical patterns in the carbonyl region, indicating the sodium ions are completely solvated and do not interact with the carboxyl moieties in the cryptate-free solution.

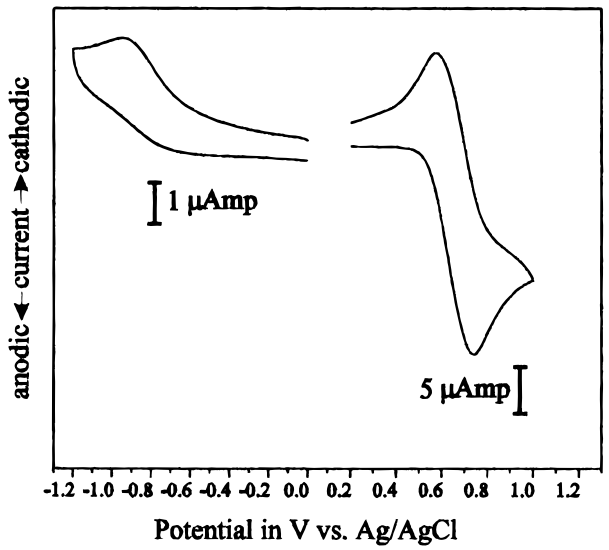

Figure 4. Cyclic voltammogram of $(CryptNa)_2Mo_6Cl_8(O_2CC_5H_4FeCp)_6$ in 0.1 M $[Bu_4N]_2BF_4$ in DMF obtained with a Pt-disk working and Pt-foil counter electrodes at a sweep rate of 0.1 V/s. Note scale difference for anodic and cathodic regions.

The electrochemical activity of the ferrocenecarboxylate ligands is retained upon coordination to the $[Mo_6Cl_8]^{4+}$ core. Cyclic voltammograms of $(cryptNa)_2[Mo_6Cl_8(O_2CC_5H_4FeCp)_6]$ in 0.1 M $[Bu_4N]BF_4$ DMF reveal a quasi-reversible oxidation wave at 0.66 V vs Ag/AgCl, assigned to the coordinated ferrocenecarboxylate/ferroceniumcarboxylate couple. A smaller irreversible reduction wave at −0.96 V is assigned to the reduction of the $[Mo_6Cl_8]^{4+}$ core to the highly unstable[41] $[Mo_6Cl_8]^{3+}$, Figure 4. The redox potential of the ferrocenecarboxylate ligand attached to $[Mo_6Cl_8]^{4+}$ is cathodically shifted 0.10 V from the oxidation of the neutral carboxylic acid, $CpFeC_5H_4CO_2H$. Only a single reduction wave is observed for the coordinated ligand, indicating the iron centers are independent and equivalent. In contrast, CVs of $[Bu_4N]_2[Mo_6Cl_8(CpMn(CO)_2CN)_6]$, which consist of $CpMn(CO)_2$ fragments coordinated to a $[Mo_6Cl_8]^{4+}$ core via bridging cyanide ligands, exhibit a very broad redox wave associated with the $Mn^{I/II}$ couple.[42] As expected, CN^- bridges more effectively couple the metal centers than the carboxylate links in $CpFeC_5H_4CO_2^-$.

The voltammetry of $(cryptNa)_2[Mo_6Cl_8(O_2CC_5H_4FeCp)_6]$ in DMSO is complicated by the absence of the return cathodic wave for the coordinated ferroceniumcarboxylate and the appearance of a new cathodic wave at 0.11 V, Figure 5A. Chronopotentiometric studies[43] on $CpFeC_5H_4CO_2H$ in acetonitrile solutions reveal two reduction waves for the oxidized product: one attributed to reduction of $[CpFeC_5H_4CO_2H]^+$ and

(39) Franolic, J. D.; Long, J. R.; Holm, R. H. *J. Am. Chem. Soc.* **1995**, *117*, 8139−8152.
(40) Nakamoto, K. *Inrared and Raman Spectra of Inorganic and Coordination Compounds*, 4th ed.; John Wiley & Sons: New York, 1986.
(41) Nocera, D. G.; Gray, H. B. *J. Am. Chem. Soc.* **1984**, *106*, 824−825.
(42) Johnston, D. H. Thesis, Northwestern University.

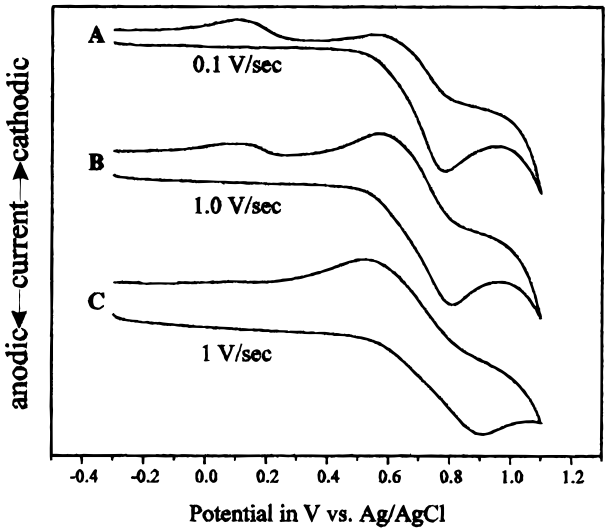

Figure 5. Cyclic voltammogram of $(CryptNa)_2Mo_6Cl_8(O_2CC_5H_4FeCp)_6$ in 0.1 M $[Bu_4N]_2BF_4$ in DMSO obtained with a working Pt-disk electrode and a Pt-foil counter electrode. Voltammograms were acquired at scan rates of (A) 0.1 V/s, (B) 1 V/s, and (C) 10 V/s.

the second to reduction of the deprotonated ferroceniumcarboxylate $[CpFeC_5H_4CO_2]$.[43] Therefore it is reasonable that the new cathodic wave at 0.11 V corresponds to reduction of uncoordinated ferroceniumcarboxylate. Upon oxidation of the pendant ferrocenyl group, the decrease in basicity of the carboxylate should make this group susceptible to dissociation. Presumably vacant coordination sites on the cluster are taken by solvent molecules. At slow scan rates (<0.05 V/s) only the cathodic wave of the uncoordinated ligand is observed, Figure 5A, while at fast scan rates (>10 V/s) the return wave of the coordinated ligand is observed with little evidence of the uncoordinated ligand, Figure 5C. Intermediate scan rates show both cathodic waves of the coordinated and free ferroceniumcarboxylate ligands, Figure 5B. The method of Nicholson and Shain[44,45] was used to determine the rate constant of the chemical reaction following the electrochemical step. A rate constant for the dissociation of the ferroceniumcarboxylate ligand of $k = 0.6\ s^{-1}$ is obtained. The ferrocene group serves as a redox switch which controls the lability of the carboxylate groups. The basicity and coordination ability of phosphines[46] and cyclic ethers[47] have been similarly controlled by modification of the ligands with redox-active ferrocene groups. In a related study, it was shown that the substitutional labilities of the axial halide ligands of $[Ta_6Cl_{12}Cl_6]^{2-}$ increase as the cluster is reduced to $[Ta_6Cl_{12}Cl_6]^{4-}$.[48]

The UV−visible spectra for $(cryptNa)_2[Mo_6Cl_8(O_2CC_5H_4FeCp)_6]$, $[Bu_4N]_2[Mo_6Cl_8Cl_6]$, and $CpFeC_5H_4CO_2H$ are shown in Figure 6. Both the $[Mo_6Cl_8]^{4+}$ cores of $[Bu_4N]_2[Mo_6Cl_8Cl_6]$ and $CpFeC_5H_4CO_2H$ display broad overlapping absorption bands in the visible or near-UV, with some weaker bands of the ferrocenecarboxylate trailing into the visible region. It is clear from Figure 6 that the absorption bands of the ferrocenecarboxylate moiety are not greatly altered upon coordination

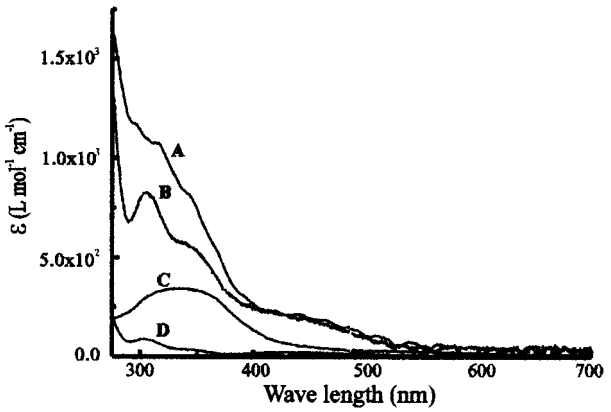

Figure 6. Absorption spectra of (A) $(CryptNa)_2Mo_6Cl_8(O_2CC_5H_4FeCp)_6$, (C) $[Bu_4N]_2[Mo_6Cl_8Cl_6]$, and (D) $CpFeC_5H_4CO_2H$ in DMF. Spectrum B is a calculated from spectra C and D with corrections for the ratio of $CpFeC_5H_4CO_2H$ to $[Bu_4N]_2[Mo_6Cl_8Cl_6]$.

to the $[Mo_6Cl_8]^{4+}$ core. However, a simple combination of the spectra for $[Bu_4N]_2[Mo_6Cl_8Cl_6]$ and $CpFeC_5H_4CO_2H$, corrected for the ratio of ferrocenecarboxylate to $[Mo_6Cl_8]^{4+}$, does not exactly reproduce the spectrum of $(cryptNa)_2[Mo_6Cl_8(O_2CC_5H_4FeCp)_6]$. This slight deviation contrasts with the absorption spectrum of $[Bu_4N]_2[Mo_6Cl_8(CpMn(CO)_2CN)_6]$, where a 10-fold increase in the intensity of the absorption band primarily associated with the manganese complex is observed upon coordination to the Mo_6 framework compared to the free ligand in solution.[34] An intensity-stealing mechanism brought about by coupling of a charge transfer band of the $[CpMn(CO)_2CN]^-$ ligand and a $[Mo_6Cl_8]^{4+}$-based transition is attributed to the increase in absorption. One requirement for the intensity-stealing mechanism is a shared orbital involved in the coupled electronic transitions.[49] Presumably, there is no common orbital available to couple the charge transfer bands of the ferrocenecarboxylate complex and the cluster-based transitions. Interestingly, the red-shifted photoluminescence observed in other $[Mo_6Cl_8X_6]^{2-}$ clusters is quenched in both $[Mo_6Cl_8(O_2CC_5H_4FeCp)_6]^{2-}$ and $[Mo_6Cl_8(CpMn(CO)_2CN)_6]^{2-}$.[41,50−52]

Conclusions

The methoxide cluster $[Mo_6Cl_8(OMe)_6]^{2-}$ is readily displaced by $CpFeC_5H_4CO_2H$ to form the new cluster $[Mo_6Cl_8(O_2CC_5H_4FeCp)_6]^{2-}$. In the solid state of $Na_2[Mo_6Cl_8(O_2CC_5H_4FeCp)_6]$, the sodium ions link neighboring clusters through the bridging carboxylate ligands, creating a one-dimensional chain containing the $[Mo_6Cl_8]^{4+}$ core. Electrochemical oxidation of the ferrocene units in DMSO is followed by facile dissociation of the oxidized ligand.

Acknowledgment. We gratefully appreciate funding from the National Science Foundation, through Grant CHE-9417250. N.P. thanks Professor J. Hupp for helpful discussions and C. Stern for collecting the X-ray data.

Supporting Information Available: Tables of positional parameters, thermal parameters, bond distances, and bond angles (10 pages). Ordering information is given on any current masthead page.

IC970816+

(43) Kuwana, T.; Bublitz, D. E.; Hoh, G. *J. Am. Chem. Soc.* **1960**, *82*, 5811−5817.
(44) Nicholson, R. S. *Anal. Chem.* **1966**, *38*, 1406.
(45) Nicholson, R. S.; Shain, I. *Anal. Chem.* **1964**, *36*, 706−723.
(46) Allgeier, A. M.; Singewald, E. T.; Mirkin, C. A.; Stern, C. L. *Organometallics* **1994**, *13*, 2928−2930.
(47) Medina, J. C.; Goodnow, T. T.; Rojas, M. T.; Atwood, J. L.; Lynn, B. C.; Kaifer, A. E.; Gokel, G. W. *J. Am. Chem. Soc.* **1992**, *114*, 10583−10595.
(48) Quigley, R.; Barnard, P. A.; Hussey, C. L.; Seddon, R. *Inorg. Chem.* **1992**, *31*, 1255−1261.
(49) Hopkins, M. D.; Gray, H. B.; Miskowski, V. M. *Polyhedron* **1987**, *6*, 705−714.
(50) Maverick, A. W.; Najdzionek, J. S.; MacKenzie, D.; Nocera, D. G.; Gray, H. B. *J. Am. Chem. Soc.* **1983**, *105*, 1878−1882.
(51) Maverick, A. W.; Gray, H. B. *J. Am. Chem. Soc.* **1981**, *103*, 1298−1300.
(52) Mussell, R. D.; Nocera, D. C. *J. Am. Chem. Soc.* **1988**, *110*, 2765−2772.